Rheological Properties of Clays

Propriétés rhéologiques des argiles

by S. MURAYAMA, Dr. Eng., Professor at the Kyoto University, Disaster Prevention Research Institute
and
T. SHIBATA, Dr. Eng., Assistant Professor at the Kyoto University, Kyoto, Japan

Summary

The viscosity of clay is assumed to be a structural viscosity, derived from statistical mechanics and based on the frequency of the mutual exchange of position between each water molecule and its void in a bond material containing soil particles. A mechanical model of clay is constructed by introducing the structural viscosity and the authors have developed a new formula relating deformation and strength of clay with this model. This formula is well adapted to explain the results of tests on compression flow, stress relaxation and long-term strength of clay.

Sommaire

Ce rapport est relatif à des recherches théoriques et expérimentales sur les propriétés rhéologiques de l'argile.

La viscosité qui intervient dans l'écoulement de l'argile est considérée comme la viscosité de structure que l'on obtient en appliquant la mécanique statistique à la fréquence des échanges mutuels de position entre les molécules d'eau et les vides dans un liant contenant des particules de sol. On établit le modèle rhéologique de l'argile en introduisant la viscosité de structure et on en déduit une nouvelle formule fondamentale relative à la déformation ou à la résistance de l'argile. Cette formule rend compte d'une manière satisfaisante des résultats des essais de fluage, de relaxation et de la résistance à long terme de l'argile.

Viscosity and mechanical model of clay

A typical flow curve for clay reveals two main stages of deformation; (1) instantaneous and (2) retarded deformation. According to T-K. TAN (1957), (1) the instantaneous deformation may be due to flexure of thin plate-like clay particles and to an increase of repulsion between the clay particles, and (2) retarded deformation may be due to the visco-elastic properties of the clay particles themselves and to the migration of water molecules.

Clay has two main properties, elastic and viscous. H. EYRING (1941) developed a formula for the viscosity of a certain liquid by statistical mechanics, proposing the existence of "holes", or irregularities in the arrangement of molecules in the liquid. In his calculation, the number of molecules with activation (or the number of unit process) of deformation was assumed to be independent of applied stress σ_l and the rate of strain $d\varepsilon_l/dt$ was expressed by :

$$\frac{d\varepsilon_l}{dt} = \frac{2\lambda nkT}{h} \exp\left(\frac{-E_0}{kT}\right) \sinh\left(\frac{\lambda}{2N}\frac{\sigma_l}{kT}\right) \qquad (1)$$

where k is Boltzmann's constant, T is the absolute temperature, h is Planck's constant, E_0 is the free energy of activation for flow, λ is the average distance between two balanced positions of molecules, n is the number of molecules with activation in series per unit length in the direction of stress and N is the number of molecules with activation in a unit area of cross section perpendicular to the direction of stress.

The viscous behaviour of clay which may be due to the exchange of position between a water molecule and a void in a bond material containing soil particles is of thixotropic character and does not conform with Eyring's theory of viscosity. The authors propose the existence of a restraining resistance σ_0 acting inside the bond and assume that N and n vary and are followed by a function of total stress σ applied to the clay skeleton which is made with elastic and viscous elements. That is,

when

$$\left.\begin{array}{ll} 0 < \sigma < \sigma_0 & n \text{ or } N = 0 \\ \sigma_0 < \sigma & n = a(\sigma - \sigma_0) \\ & N = b(\sigma - \sigma_0) \end{array}\right\} \qquad (2)$$

where a and b are constants.

Substituting Eq. (2) for Eq. (1), we obtain the following equation relating the rate of strain of the bond $d\varepsilon_b/dt$ with the stress on the bond σ_b by changing the suffix l in Eq. (1) with suffix b.

$$\frac{d\varepsilon_b}{dt} = A_b(\sigma - \sigma_0) \sinh\left(\frac{B_b\ \sigma_b}{\sigma - \sigma_0}\right)$$

and

$$\left.\begin{array}{l} A_b = \dfrac{2\lambda akT}{h} \exp\left(\dfrac{-E_0}{kT}\right) \\ B_b = \dfrac{\lambda}{2bkT} \end{array}\right\} \quad \ldots\ (3)$$

Hence the apparent coefficient of viscosity of the bond is represented as

$$\eta_b = \frac{1}{A_b \sinh\left(\dfrac{B_b\ \sigma_b}{\sigma - \sigma_0}\right)} \qquad (4)$$

The authors also propose that Eq. (2) is valid only within a certain limit of σ, and that, if applied total stress σ overcome this limit, bonds will start to break to bringing clay failure. An applied stress which causes bond breakage is defined as the upper yield value σ_u.

The elastic constant E (E_1 or E_2) of the elastic elements shown in Fig. 1 is assumed to be unchanged unless the applied total stress is greater than the preconsolidation stress σ_c, because the orientation of clay particles is considered to be

affected only by the total stress exceeding σ_c. The authors obtained a relationship between the elastic modulus E (E_1 or E_2 of the model shown in Fig. 1) and the applied stress σ as follows for the region of $\sigma > \sigma_c$.

$$E = \frac{\sigma}{\frac{\sigma_c}{E_c} + \frac{1}{E'} \log \frac{\sigma}{\sigma_c}} \quad \ldots\ldots (5)$$

where E_c and E' are constants.

The mechanical model shown in Fig. 1 was developed to explain the viscosity, elasticity and internal resistance of clay (1956).

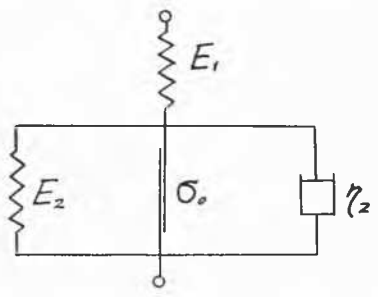

Fig. 1 Rheological model for clays.
Modèle rhéologique pour argiles.

It consists of a series coupling of a spring element E_1, and a modified Voigt element (E_2, σ_0, η_2), the dashpot of the latter representing the structural viscosity expressed in Eq. (4).

The relationship between the strain of the modified Voigt element ε_2, and the applied stress on the dashpot σ_2 is represented as follows, by changing the suffix b in Eq. (3) with suffix 2.

$$\frac{d\varepsilon_2}{dt} = A_2(\sigma - \sigma_0) \sinh \left(\frac{B_2\sigma_2}{\sigma - \sigma_0} \right) \quad \ldots\ldots (6)$$

Clay specimen and compression plastometer

Undisturbed clay samples used for the tests were obtained from the alluvial clay stratum in Osaka City with the aid of a thin-walled sampler with a stationary piston. This clay is normally consolidated, and its physical properties are as follows : specific gravity ; 2·67, L.L. ; 83 — 63 per cent ; P.L. ; 36 — 25 per cent, natural moisture content ; 92 — 58 per cent, degree of saturation ; 100 per cent.

Fig. 2 shows the compression plastometer which consists of a triaxial testing unit and a recording 1-1 and controlling-unit. Load imposed on the loading rod and its displacement can be automatically and continuously recorded electrically. With this plastometer, various types of compression tests can be performed automatically.

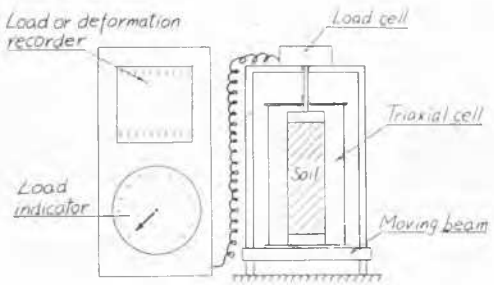

Fig. 2 Schematic arrangement of compression plastometer.
Schéma d'un plasticimètre à compression.

The clay specimen (8·5 cm in height and 3·5 cm in diameter), placed in the triaxial cell, was protected by a rubber membrane ; the top porous plate on the specimen was connected to the drainage system and the lower plate to the pore-pressure measuring system.

To avoid the effects of stress-history, each fresh specimen of the same clay was used for each test.

Flow mechanism of clay

Flow Characteristics. — The relationship between total strain ε and time t, can be obtained by solving the following simultaneous equations (c.f. Fig. 1),

$$\varepsilon = \varepsilon_1 + \varepsilon_2$$
$$\sigma = \varepsilon_1 E_1$$
$$\sigma = \varepsilon_2 E_2 + \frac{(\sigma - \sigma_0)}{B_2} \sinh^{-1} \left\{ \frac{1}{A_2(\sigma - \sigma_0)} \frac{d\varepsilon_2}{dt} \right\} + \sigma_0 \quad \ldots\ldots (7)$$

If

$$0 < \varepsilon_2 < \frac{(\sigma - \sigma_0)}{2B_2E_2} (2B_2 - 1) \quad (8)$$

ε is given approximately as

$$\varepsilon = \frac{\sigma}{E_1} + \frac{(\sigma - \sigma_0)}{E_2} + \frac{(\sigma - \sigma_0)}{B_2E_2} \log \frac{A_2}{2} B_2E_2t \quad (9)$$

If ε_2 beyond the limits of relation (8), viz.

$$\varepsilon_2 > \frac{(\sigma - \sigma_0)}{2B_2E_2} (2B_2 - 1) \quad (10)$$

we obtain at $t \to \infty$

$$\varepsilon_{t\to\infty} = \frac{\sigma}{E_1} + \frac{(\sigma - \sigma_0)}{E_2} \quad (11)$$

Eqs. (9) and (11) show that the flow strain of clay ε is proportional to the logarithm of time t at first but should approach to $\varepsilon_{t\to\infty}$ as shown in Fig. 3.

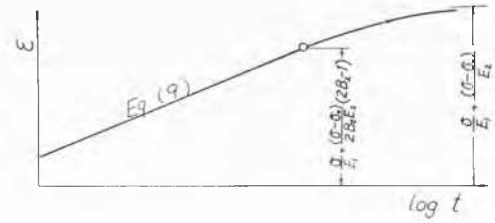

Fig. 3 Relationship between flow strain and time.
Relation entre la déformation et le temps.

Performing long term anisotropic consolidation tests with the plastometer, axial displacement, pore water pressure at the lower surface of the specimen and the volume of water expelled from the specimen were measured.

Typical results are illustrated in Fig. 4. Fig. 4 (a), in which axial strain is plotted against the logarithm of time t, shows that the secondary compression curve (continuous line) exhibits the purely compressive flow character of clay. As shown in Fig. 4 (b) and (c), the effect of pore-water movement and pore-water pressure on flow behaviour may be negligible. Fig. 5 shows the strain-time curves (continuous lines) obtained by these tests and these curves reveal that the flow strain ε increases proportionately with the logarithm of time t as represented by Eq. (9).

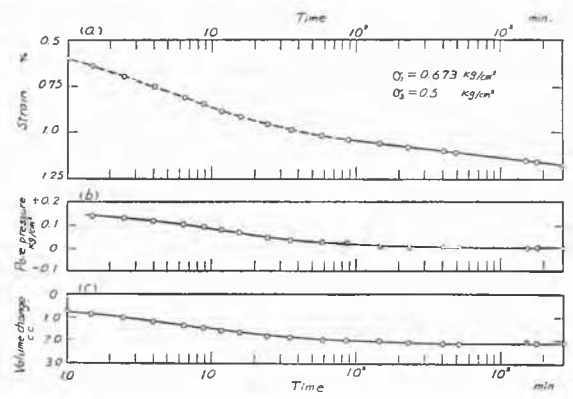

Fig. 4 A typical example of flow test results : a) flow strain ; b) pore water pressure ; c) volume change.
Un exemple typique des résultats d'écoulement : a) déformation ; b) pression interstitielle ; c) variations de volume.

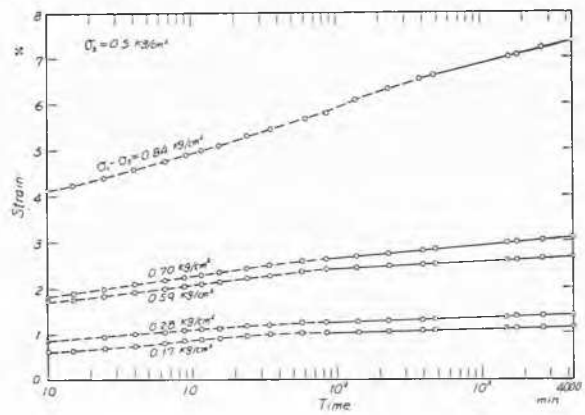

Fig. 5 Deformation — time diagram.
Graphique temps — déformation.

Strain rate characteristics. — From Eq. (9) the strain-rate is given by

$$\frac{d\varepsilon}{d\log t} = \frac{(\sigma - \sigma_0)}{B_2 E_2} \qquad \ldots . \quad (12)$$

Therefore, the relationship between the strain-rate $d\varepsilon/d \log t$ and its applied stress σ (so-called D — τ curves) should be represented by a straight line within the stress range from σ_0 to the upper yield value.

In Fig. 6, $d\varepsilon/d \log t$ obtained by flow tests is plotted against its applied deviator stress $(\sigma_1 - \sigma_3)$. Fig. 6 shows that the curve is linear within the stress range up to $(\sigma_1 - \sigma_3) = 0{\cdot}7$ kg/cm^2. The abscissa of the point of intersection of the curve with the σ — axis gives the lower yield value σ_0, below which no flow deformation takes place. The stress corresponding to the first inflection point of the curve gives the upper yield value σ_u, and this value is the maximum stress which can exerted for a long time without failure.

Thermal effect on flow. — Substituting B_2 of Eq. (3) into Eq. (12), and neglecting σ_0 we obtain

$$\frac{d\varepsilon}{d\log t} \doteq \frac{2bk\sigma}{\lambda E_2} T \qquad (13)$$

Eq. (13) shows that $d\varepsilon/d \log t$ and temperature T are directly proportional if the applied stress σ is constant.

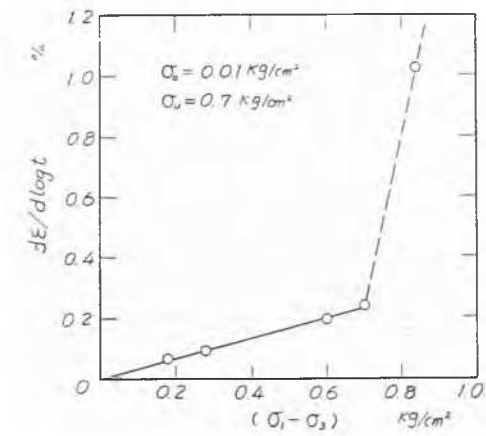

Fig. 6 Relation between $d\varepsilon/d \log t$ and stress.
Relation entre $d\varepsilon/d \log t$ et contrainte.

The result of tests on the thermal effect of compression flow of clay is shown in Fig. 7. In Fig. 8, each $d\varepsilon/d \log t$ obtained from Fig. 7 is plotted against the absolute temperature T for a constant value of σ. This figure proves the validity of Eq. (13).

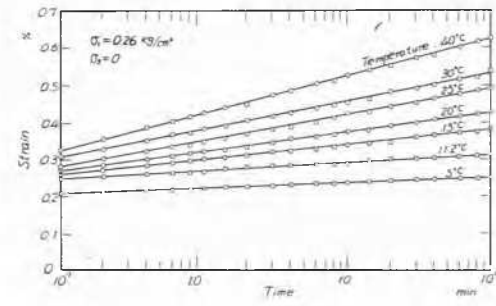

Fig. 7 Deformation related to time.
Graphique temps — déformation.

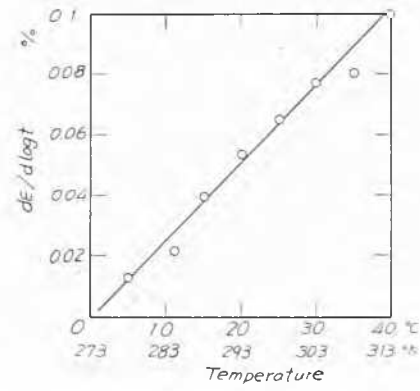

Fig. 8 Rate of flow as a function of temperature.
Vitesse d'écoulement en fonction de la température.

Stress relaxation of clay

The relaxation of stress in clay under constant initial deformation, viz. the relation between total stress σ and time t can be obtained by solving the simultaneous Eq. (7) under the condition of $\varepsilon = \varepsilon_0$ (const.) at $t = 0$. Approximate result is given as

$$\int_{u_0}^{u} \frac{1}{u}\exp(u)\,du = C \cdot t$$

where

$$\left.\begin{aligned} u_0 &= B_2 \frac{E_2}{E_1} \\ u &= \frac{B_2 E_2}{(\sigma - \sigma_0)}\left(\varepsilon_0 - \frac{\sigma_0}{E_1}\right) \\ C &= \frac{A_2}{2} E_1 \exp\left\{B_2\left(1 + \frac{E_2}{E_1}\right)\right\} \end{aligned}\right\} \quad (14)$$

and at $t \to \infty$

$$\sigma_{t\to\infty} = \frac{E_1 E_2}{E_1 + E_2}\varepsilon_0 \quad (15)$$

The results of the stress — time relationships numerically calculated by Eq. (14) applying model constants found by the experiments shown in Fig. 10 (i.e. $E_1 = 48{\cdot}0$ kg/cm^2, $E_2 = 34{\cdot}3$ kg/cm^2, $B_2 = 5{\cdot}0$) are shown in Fig. 9 for various values of initial strain ε_0, and these calculated curves are represented by approximate straight lines on the semi-logarithmic paper. When the internal stress is entirely transmitted to the spring elements E_1 and E_2 in the mechanical model shown in Fig. 1, stress relaxation ceases.

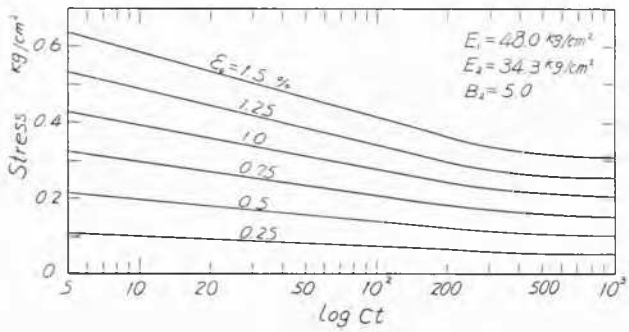

Fig. 9 Calculated stress-relaxation curves.
Graphiques contraintes-relaxation.

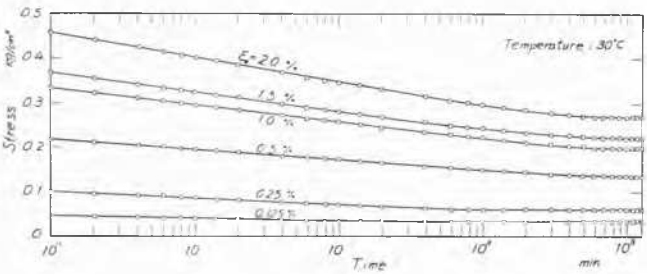

Fig. 10 Relaxation of stresses.
Relaxation des contraintes.

The result of stress relaxation test under the undrained condition obtained by the plastometer shown in Fig. 2 is given in Fig. 10, this shows that stress decreases proportionately with the logarithm of time and finally approaches to a finite value like as shown in Fig. 9.

Long-term strength

If any constant stress exceeding the upper yield value is applied to clay, the clay will fail after it flows. Since the authors defined such stress that exceeds the upper yield value the long-term strength, the long-term strength does not mean a definite value.

When the stress exceeding the upper yield value is applied to clay, the rate of flow strain shows a marked increase as compared with that at the stress lower than the upper yield value. This fact is considered to be due to the successive breaking of bond between clay particles caused by the application of external stress exceeding the upper yield value. Therefore, if the number of such bonds per unit cross sectional area perpendicular to the direction of the applied stress of clay is N_b, failure will take place when the number of remaining bonds becomes zero.

Since the ratio of number of activating bonds per unit time dN_b/dt and total bonds N_b is equal to the frequency of activation of one bond per unit of time, if the broken bonds are repaired, the rate of breaking of such bonds at constant stress σ is written as follows :

$$-\frac{1}{N_b}\frac{dN_b}{dt} = \frac{2kT}{h}\exp\left(\frac{-E_0}{kT}\right)\sin h\left(\frac{\lambda\sigma_2}{2N_b kT}\right) \quad (16)$$

where σ_2 is the stress applied on the dashpot shown in Fig. 1, and $\sigma_2 = \sigma - \sigma_0 - \varepsilon_2 E_2$.

When the stress is near that of failure, the elasticity of clay becomes negligible and the lower yield value σ_0 is very small compared with the applied stress σ, hence $\sigma_2 \fallingdotseq (\sigma = \sigma_0) \fallingdotseq \sigma =$ const. Therefore, when the intensity of applied stress σ is higher or the repair of the bonds does not occur, Eq. (16) becomes

$$-\frac{1}{N_b}\frac{dN_b}{dt} = \frac{kT}{h}\exp\left(\frac{-E_0}{kT}\right)\exp\left(\frac{\lambda\sigma}{2N_b kT}\right) \quad (17)$$

Approximate solution of Eq. (17) is given as

$$\log_{10} t_f = \log_{10}\frac{h}{kT} + \frac{E_0}{2{\cdot}3kT} - \frac{\lambda\sigma}{4{\cdot}6N_{b0}kT} \quad \cdots \quad (18)$$

where t_f is the time when N_b becomes zero or the time lapse necessary to the flow failure, N_{b0} the initial number of bonds per unit area of clay.

Eq. (18) represents the linear relation between the long-term strength σ and the logarithm of the time to failure t_f.

Fig. 11 illustrates the flow curves and those points where failure took place, obtained by unconfined compression tests under constant stress σ exceeding the upper yield value. Fig. 11

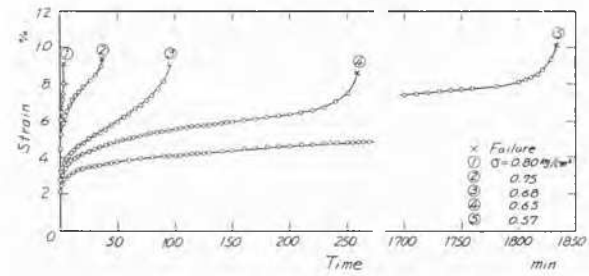

Fig. 11 Flow curves for clay.
Graphique de l'écoulement de l'argile.

shows that every flow strain value at failure is almost the same irrespective of the applied stress, but the higher the intensity of the long-term strength, the shorter will be the time at which flow failure takes place. The results of this test and another such tests for flow failure are given in Fig. 12. As the experimental data are in close agreement with each straight

line on a semi-logarithmic scale, each relationship between σ and t_f is quite satisfactorily expressed by Eq. (18), and the tangent of the slope of each line should be equal to the values of $\lambda/4{\cdot}6N_{b0}kT$.

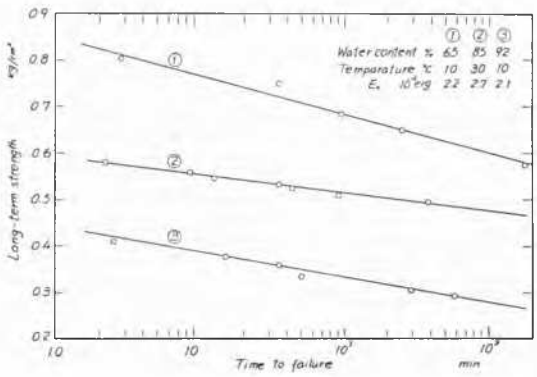

Fig. 12 Relationship between the long-term strength and the time elapsed until failure occurs.
Relation entre la résistance à long terme et le temps écoulé jusqu'à la rupture.

If $\log_{10} t_f$ at $\sigma = 0$ is written as $\log_{10} t_{f\cdot i}$, the actual value of $\log_{10} t_{f\cdot i}$ can be obtained by extrapolating the straight ine part of $\sigma - t_f$ line. As the cquation of $\log_{10} t_{f\cdot i}$ is given by

$$\log_{10} t_{f\cdot i} = \log_{10} \frac{h}{kT} + \frac{E_0}{2{\cdot}3kT} \tag{19}$$

the value of activation free energy E_0 can be computed from Eq.(19). E_0 thus calculated are tabulated in Fig. 12 and have order of 10^{-12} erg respectively.

Addendum

In the above, the authors refer only to some results which can be deduced from their formula. In addition, some problems of secondary compression, consolidation by dynamic stress, the flow effects of repetitional load and a new measuring method for determining the upper yield value of clay and preconsolidation stress have been investigated, and some of them will be reported in subsequent papers.

References

[1] Tan Tjong Kie (1957). Rheological process in frozen soils and dense clays.

[2] Vialov, S. S. and Skibitsky, A. M., *Proc. 4th International Conference on Soil Mechanics and Foundation Engineering*, vol. 3, pp. 87-89.

[3] Glasstone, S., Laidler, K. J. and Eyring, H. (1941). The theory of rate process, New York, p. 477.

[4] Murayama, S. and Shibata, T. (1956). On the rheological characters of clay, *Transactions of the Japan Society of Civil Engineers*, No. 40, pp. 1-31.